Histological and functional assessment of the motor system in a non-human primate affected by Polymicrogyria.

Eric Schmidlin1,*, Patrick Freund1*, Christophe Jouffrais1, 2*, Patrizia Wannier-Morino1, Marie-Laure Beaud1, Eric M. Rouiller1 and Thierry Wannier1

* The first three authors contributed equally to the study.

(1) Unit of Physiology and Program in Neurosciences, Department of Medicine, Faculty of Sciences, University of Fribourg, Chemin du Musée 5, CH-1700 Fribourg, Switzerland.

(2) IRIT, Université de Toulouse and CNRS, 133 route de Narbonne, 31062 Toulouse cedex 9 France

Poster C62 Session P083

Introduction

Polymicrogyria (PMG) is a developmental malformation of the brain. It is defined as the presence of multiple small gyri with abnormal lamination of the cerebral cortex. This rather common brain malformation in human patients affects also non-human primates but presents several forms according to the extent of the affected regions of the brain, the extent being directly related to the severity of the symptoms. This disease presents a large range of functional consequences: from no impairment to severe epilepsy, motor and cognitive deficits.

We discovered this malformation in a monkey which was involved in experiments requiring the learning of a complex bimanual motor task.

In this study, we confront the observations obtained in this particular animal with observations made in a series of animals that did not present any malformation or dysfunction.

Results

Anatomy

Figure 1

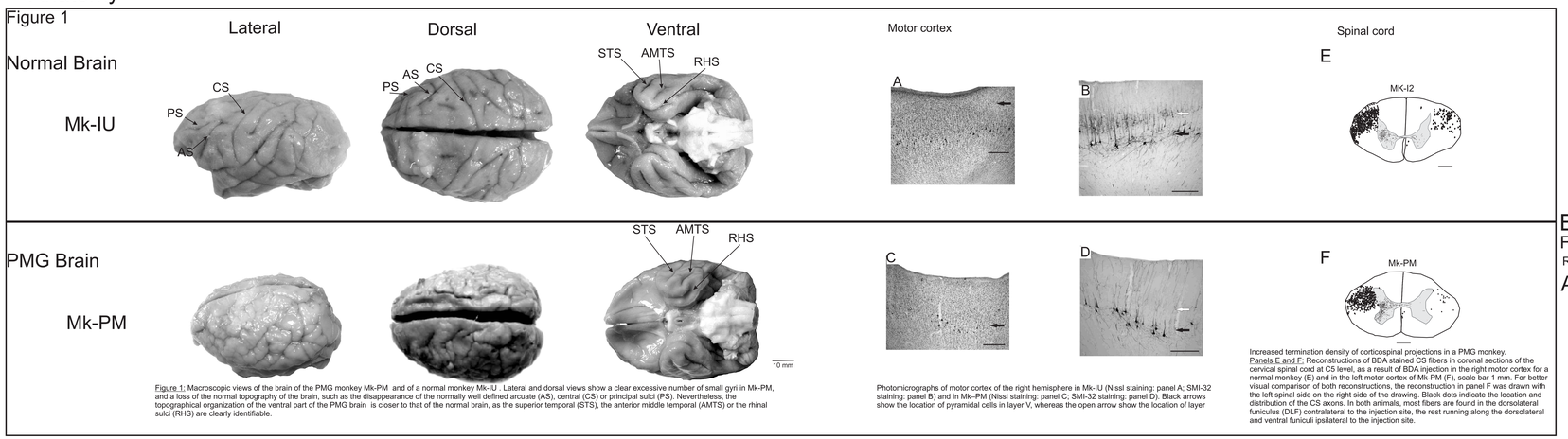

Figure 1: Macroscopic views of the brain of the PMG monkey Mk-PM and of a normal monkey Mk-IU . Lateral and dorsal views show a clear excessive number of small gyri in Mk-PM, and a loss of the normal topography of the brain, such as the disappearance of the normally well defined arcuate (AS), central (CS) or principal sulci (PS). Nevertheless, the topographical organization of the ventral part of the PMG brain is closer to that of the normal brain, as the superior temporal (STS), the anterior middle temporal (AMTS) or the rhinal sulci (RHS) are clearly identifiable.

Photomicrographs of motor cortex of the right hemisphere in Mk-IU (Nissl staining: panel A; SMI-32 staining: panel B) and in Mk-PM (Nissl staining: panel C; SMI-32 staining: panel D). Black arrows show the location of pyramidal cells in layer V, whereas the open arrow show the location of layer

Increased termination density of corticospinal projections in a PMG monkey. Panels E and F: Reconstructions of BDA stained CS fibers in coronal sections of the cervical spinal cord at C5 level, as a result of BDA injection in the right motor cortex for a normal monkey (E) and in the left motor cortex of Mk-PM (F), scale bar 1 mm. For better visual comparison of both reconstructions, the reconstruction in panel F was drawn with the left spinal side on the right side of the drawing. Black dots indicate the location and distribution of the CS axons. In both animals, most fibers are found in the dorsolateral funiculus (DLF) contralateral to the injection site, the rest running along the dorsolateral and ventral funicuil ipsilateral to the injection site.

Figure 2

Reconstruction of frontal Nissl-stained sections in PMG monkey

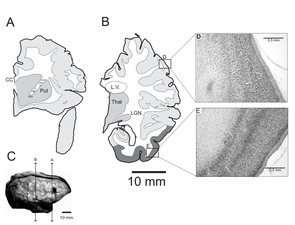

Figure 2: Panels A and B: Location of the healthy looking cortex versus the disordered looking cortex in the right hemisphere at two rostrocaudal levels. Sub-cortical structures, such as the thalamus (Thal.), the lateral geniculate nucleus (LGN), the putamen (Put) or the corpus callosum (CC) are visible and they do not present conspicuous abnormalities, but the lateral ventricle (L.V.) is enlarged. Panel C: Photograph of the cortex in Mk-PM with the position of the sections depicted in panels A and B. Panels D and E: The cortical organization in layers is lost in the parietal lobe in the somatosensory cortex (D) but normal in the inferior temporal lobe (E).

Figure 3

Abnormalities in cortical organization in PMG monkey

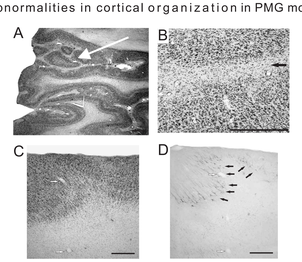

Figure 3: Panel A: Photomicrograph of a Nissl stained section demonstrating the disorganization of the microgyral cortex. The layered organization is irregular and anomalous, with the formation of small islets (arrow). Panel B: Photomicrograph showing the lack of lumen and of pia between two facing portions of cortex in a sulcus. This results in the fusion of both layers I in a unique strip of white matter (black arrow). Panel C: Photomicrograph of a Nissl stained section showing the absence of well defined laminar organization. Panel D: Photomicrograph of a SMI-32 stained section adjacent to the section presented in B. Note that the SMI-32 positive neurons occupy positions in the cortex which vary strongly with regard to its distance to the cortex surface (black arrows). White arrows in C and D indicate the same blood vessels. Scale bar: 500 microns.

Figure 4

Analysis of the red nucleus in PMG monkey

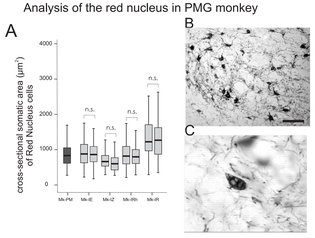

Figure 4: Panel A: Distribution of SMI-32 neurons size in the red nucleus, pars magnocellularis (RNm) of the PMG monkey (dark grey) and in four normal animals (light grey) represented in the form of box and whiskers plots. For the PMG animal, measurements could only be done in the left RNm. Somatic area of cells in RN in Mk-PM can be compared to normal animals Mk-I1 to I3. Panel B: SMI-32 staining of the red nucleus pars magnocellularis in the PMG monkey. The general structure of the nucleus is comparable to that observed in normal animals. Panel C: abnormal accumulation of vesicles in a SMI-32 positive RNm neuronin Mk-PM.

Figure 5

Somatic cross-sectional areas of SMI-32 positive neurons in layer V in motor cortex

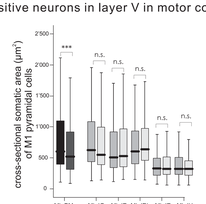

Figure 5: Box and whisker plots showing the distribution of somatic cross-sectional areas of SMI-32 positive neurons in layer V in motor cortex for Mk-PM (dark grey) and five normal monkeys (light grey). In the box and whisker plots, the thick horizontal line in the box corresponds to the median value, whereas the top and bottom of the box are for the 75 and 25 percentile values respectively. The top and bottom extremities of the vertical lines on each side of the box are for the 90 and 10 percentile values, respectively. Mk-PM exhibited a significant inter-hemispheric difference of cross-sectional soma area (***p<0.0001; Mann and Whitney test), whereas in the normal monkeys the difference was not statistically significant (n.s. =p>0.05; Mann and Whitney test).

Figure 6

Increased termination density of corticospinal projections in a PMG monkey.

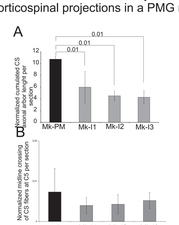

Figure 6: In comparison to normal animals, few corticospinal (CS) fibers were found in the gray matter ipsilateral to the BDA injection site, in Mk-PM. Panel A: Normalized arbor length of CS projections in the cervical grey matter in the PMG animal (black) and in three normal animals (grey). The extension of neurites in the grey matter was significantly larger in the PMG animal. Panel B: Number of midline crossing CS fibers at cervical level C5. The number of fibers crossing the midline and terminating in the opposite grey matter was normalized by dividing it by the total number of labeled CS fibers present in the white matter (see methods for detail).

Methods

The data were derived from eleven adults (3-8 years old) macaque monkeys (Macaca mulatta and fascicularis, of either sex, weighing from 3.0 to 5.0 kg, see Table 1).

Anatomy:

For anatomical investigation, we used standard paraformaldehyde perfusion technique, including Nissl stained sections methods.

To stain the corticospinal projections, we used intracortical injections of Biotin Dextran Amin (BDA) in the primary motor cortex hand area localized using intracortical microstimulation (ICMS) in the left hemisphere.

Particular cortical staining using an antibody specifically directed against neurofilaments (SMI-32).

Morphometric analysis using Neurolucida© software allowed the measure of the cross sectional sections of SMI-32 stained pyramidal neurons in motor cortex and in the Red Nucleus.

Measure of the midline crossing BDA labeled corticospinal tract fibers at cervical level.

Behavior:

Reach and grasp drawer task: four different visual stimuli corresponding each to a particular task: opening of a drawer and picking a food reward unimanually or bimanually and starting or using the left or right hand.

Defined time epochs:

Reach: from 'hand release of the pads 'to 'grasp knob of the drawer'

Reach2: from 'grasping hand movement onset' to 'enter drawer' in the bimanual task

Pull: from 'grasp knob' to 'drawer fully open'

Grasp: from 'drawer open' to 'hand out of drawer

'Intracortical microstimulation (ICMS) consisted in penetration of a microelectrode delivering train (12 pulses) of electric stimulation to elicit muscle contraction in the contralateral forelimb or face

Behavior

Figure 7

Reaction time

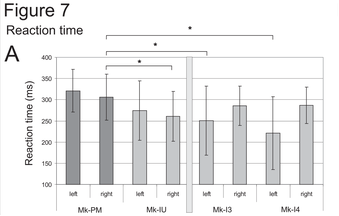

Figure 7 A: Reaction times (RT) for both hands in the behavioral unimanual task for the 4 animals involved in the behavioral reach and grasp drawer task. Statistical comparison accross animals (Mann and Whitney) are for the hand with the shortest RT's.

Movement time

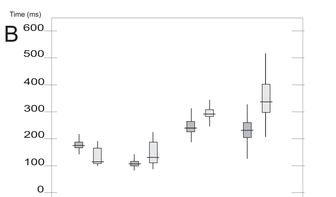

Figure 7 B: Box plots and statistical analysis (Mann-Whitney) of the movements times in Mk-PM (dark grey) and Mk-IU (light grey) during the reach and grasp drawer task.

Figure 8

Intracortical microstimulation

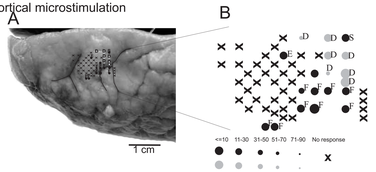

Figure 8: Panel A: Left frontal lobe region of the brain of the PMG animal with the map of the sites where intracortical microstimulation (ICMS) has been performed. Note the difficulty to identify the central sulcus and the precentral gyrus. Panel B: Map of the sites where ICMS has been performed, with indications on the location of the observed movement and of the minimal current required to elicit the movement. D: digit, F: face, E: elbow and S: shoulder. X: No response at 80 microamps of stimulation intensity.

Results

Anatomy:

Macroscopic view of the brain shows PMG malformation present particularly in the frontal, parietal and occipital lobes. No clear landmarks such as the central sulcus are identifiable.

Microscopic view shows a disorganization of the cortical layers and changes in the grey matter / white matter distribution in the affected gyri. The cortical cytoarchitecture is also affected: absence of SMI-32 stained pyramidal neurons in layer III.Increased presence of corticospinal axon arbors in the spinal grey matter was the only significant alteration observed, including a tendency for an enhanced midline crossing at the same cervical level.Analysis of the magnocellular part of the Red Nucleus shows a normal number of cells but marked intracellular abnormalities such as numerous possible nuclear vesicles.

Function:

Intracortical microstimulation in the supposed primary motor cortex in the PMG monkey shows a normal sensitivity of the cortical motor neurones to low threshold stimulation trains and the normal presence of sites eliciting finger movements and other parts of the forelimb or face.

Behavior:

Compared to other animals. the reaction time in the PMG monkey was significantly increased. In opposite, the timing of movements such as reaching or grasping were not significantly affected in the PMG monkey.

Conclusion:

PMG monkey with consequent largely distributed brain malformations suffered from a moderate of behavioral impairment, essentially limited to a delay in movement initiation (increased RT) in the reach and grasp drawer task.

Discussion

Dramatic macro- and microscopic changes in a monkey brain confirm the diagnosis of PMG in this single case. The polymicrogyria should be classified as a bilateral frontoparietal polymicrogyria (BFPP).

The size distribution of layer V pyramidal neurons in the PMG macaque is not distinguishable from that found in normal macaques, but a significant size difference was found between the left and right hemisphere pyramidal neurons in the PMG animal.

Interestingly, in opposite to what is observed in normal monkeys, no SMI-32 positive layer III pyramidal neurons were present in the motor cortex of the PMG animal.

Corticospinal tract fiber distribution was similar to that of normal animals, which indicates that the basic structure of the corticospinal tract is preserved in the PMG monkey. However, as few fibers end in the gray matter on the side ipsilateral to the BDA injection and as the number of fibers crossing the midline at cervical level was significantly increased in the PMG animal, the CS fibers seem to have a higher propensity to innervate the side contralateral to the injection as is normally the case. These minor structural changes may be related to observations which indicate that 25% of PMG patients suffer from hemiparesis.

Interestingly, despite the marked cortical modifications changes, the corticospinal projections do not seem to be affected by this malformation, and even more interestingly, no particular behavioral changes were suspected during the experimental paradigm.The behavioral difference between the PMG monkey and the normal monkey both engaged in the same reach and grasp drawer task is thus restricted to the RTs, significantly prolonged in the PMG monkey.

Overall, these data suggest that the PMG pathology may have affected some cortico-cortical connections (crucial for attention), but not the corticospinal projection as indicated by normal motor control in a well trained behavioral task

Table 1

Name	Mk-PM	Mk-IU	Mk-IE	Mk-IZ	Mk-IRh	Mk-IR	Mk-IG	Mk-I1	Mk-I2	Mk-I3	Mk-I4
gender	♂	♂	♀	♂	♀	♀	♂	♂	♂	♂	♂
species	M.Mulatta	M.Mulatta	M.Fascicularis	M.Fascicularis	M.Mulatta	M.Mulatta	M.Mulatta	M.Mulatta	M.Fascicularis	M.Mulatta	M.Mulatta
age	5	9	4	8	5	4	6	4	8	6	6
BDA staining	yes						yes	yes	yes	yes	
Behavior testing	yes	yes						yes	yes	yes	yes
SMI-32 staining	yes	yes	yes	yes	yes	yes	yes	yes	yes	yes	

Acknowledgements

The authors wish to thank the technical assistance of Georgette Fischer, Véronique Moret, Françoise Tinguely, Christiane Marti, Monika Bennefeld and Christine Routin (histology and behavioral evaluations), Josef Corpataux, Bernard Bapst, Laurent Bossy and Bernard Morandi (animal house keeping), André Gaillard (mechanics), Bernard Aebischer (electronics), Laurent Monney (informatics).